On the indentation recovery and fleeting hardness of polymers

Catherine A. Tweedie and Krystyn J. Van Vliet[a)]
Department of Materials Science and Engineering, Massachusetts Institute of Technology, Cambridge, Massachusetts 02139

(Received 23 January 2006; accepted 2 August 2006)

Accurate mechanical characterization of viscoelastoplastic materials in small volumes is required for the development of polymeric thin film, nanocomposite, and biomedical applications. Instrumented indentation-based approaches are increasingly implemented to quantify the resistance to permanent deformation of such systems via time-independent analyses. Here, we quantify the significant post-indentation recovery of several bulk polymers via time-lapsed scanning-probe microscopy under ambient conditions, indicating up to 80% recovery of both indentation depth and volume within 48 h. This viscoelastic response demonstrates that indentation hardness values for these polymers are accurate within 10% for less than 5 min to 3.5 days post-indentation, neglecting any other analytical or experimental errors. Further, although the extent and rates of volumetric recovery depend strongly on loading history and polymer structure/physical properties, deformation resistance inferred from indentation hardness does not quantitatively or qualitatively predict recoverable work or residual deformation of polymer surfaces.

I. INTRODUCTION

Mechanical characterization of small-volume and thin film polymers via instrumented indentation is frequently applied to estimate mechanical properties such as the Young's modulus, E, and semi-quantitative metrics of resistance to plastic deformation such as indentation hardness, H_i.[1] Despite the prevalence of such experiments in the literature and in industrial application, the attainment and interpretation of polymer nanoindentation is often based on a framework developed for time-independent materials. That is, load-displacement data are analyzed following closed-form, semi-empirical equations based in contact mechanics for linear elastic, von Mises yielding materials such as metals.[2–4] This compromise is accepted for convenient metrics such as H_i without a quantitative understanding of post-indentation polymer recovery rates at room temperature, which would appraise the applicability of H_i:

$$H_i = \frac{P_{max}}{A_c(h_c)} \quad , \tag{1}$$

where P_{max} is the maximum load applied during indentation and $A_c(h_c)$ is the calculated contact area at that load.[5] Indentation hardness is therefore dependent on the contact depth, h_c, which is a function of the maximum depth at complete unloading of the surface, h_o.[5]

Recovery of polymer surfaces has been the focus of several previous studies.[6–12] Lorenzo et al.[8] related the change in uninstrumented Vickers microhardness depth ($h_{max} \geqslant 10$ μm) determined through interference microscopy post-indentation to variations in weight-average molecular weight, M_w, and %-crystallinity for bulk polyethylene. The authors observed a negative correlation between extent of indentation depth recovery and both %-crystallinity and yield stress. However, these experiments were limited to discrete depth measurements and could not be extended to measure changes in volumetric recovery. Similarly, Low noted for polyacrylics that the diagonal lengths, D, of a Vickers (square pyramidal) microhardness impression remained approximately fixed when measured via optical microscopy over 48 h post-indentation, despite the observed inward sidewall bowing or "pin cushioning" effect.[7] This temporal consistency in D was used to justify Vicker's microhardness, H_V, as a valid metric for polymer mechanical characterization. Of course, although this does satisfy the procedural aspects of measuring microhardness through optical observation of D post-testing, instrumented indentation hardness H_i computed from the continuously measured load-displacement ($P - h$) response is intended to quantify the average effective stress required to plastically deform the

a)Address all correspondence to this author.
e-mail: krystyn@mit.edu
DOI: 10.1557/JMR.2006.0377

material—a metric with units of stress that is load- and loading time-dependent for polymers.[13] Thus, the constancy of position of indentation apices and diagonals measured between those apices need not be synonymous with resistance to plastic deformation of the entire indentation-deformed polymeric volume.

Chang et al. have considered the finite recovery of microscale contact deformation as a function of elevated temperature to determine relaxation or recovery kinetics of amorphous polymers such as polystyrene.[6,10–12] By recording a contact profilometry line scan through the Vickers microindentation depth minima at discrete temperatures up to 55 h post-indentation, the authors concluded that microindentations imposed at room temperature recovered many times faster than those imposed at elevated temperature during a subsequent annealing phase[12] and, as expected, that indentation depth minima recovery rates changed most rapidly near the glass transition temperature.[6]

In the present work, continuous mapping of the evolving indentation topography at room temperature provides fuller understanding of confined polymer recovery, enabling a definitive evaluation of indentation hardness characterization of polymers and a quantitative determination of viscoelastic recovery at deformed surfaces.

II. EXPERIMENTAL

A. Materials

The volumetric recovery of three bulk, engineering polymers post-indentation was considered: polyethylene (PE), polycarbonate (PC), and polystyrene (PS). The glass transition temperatures, T_g, the weight-average molecular weights, M_w, and the polydispersity indices (PDI) were as follows for the three polymers: PE (T_g = −30 °C, M_w = 85,195 g/mol, PDI = 3.10), PC (T_g = 145 °C, M_w = 18,000 g/mol, PDI = 1.57), and PS (T_g = 103 °C, M_w = 248,670 g/mol, PDI = 3.14). Indentation experiments were conducted at ambient temperature T_a = 22 °C, pressure, and humidity RH < 50%. Note that $T_a > T_g$ of PE with a melting temperature T_m of ~125 °C (68% crystalline, as quantified by wide-angle x-ray diffraction; data not shown), but that $T_a < T_g$ for PS and PC (fully amorphous). These samples were obtained from DuPont as smooth discs (4–5 nm root mean square surface roughness, as measured via scanning-probe microscopy; MFP3D, Asylum Research, Santa Barbara, CA) processed via injection molding into a polished aluminum mold. The T_g was measured via differential scanning calorimetry[14] as reported by the manufacturer and confirmed in the present study, and M_w was determined by the manufacturer via gel permeation chromatography.

These polymers provide a wide range of mechanical response: the varied monomer composition among the three polymers results in persistence lengths, L_p, the length scale over which a polymer chain is effectively rigid,[15] which vary by a factor of six ($L_{p,\,PC}$ = 3 nm,[16] $L_{p,\,PS}$ = 0.9 nm,[15] and $L_{p,\,PE}$ = 0.5 nm[17]). All of these polymer chains are relatively flexible, as can be characterized by $\chi \ll 1$, where χ is L_p normalized by polymer chain contour length L_c. However, the values of χ for these polymers varied by orders of magnitude [3.64×10^{-2} (PC), 1.25×10^{-3} (PS), and 1.25×10^{-4} (PE)].[18–20] Thus, PE is expected to exhibit greater intermolecular motion, despite being semi-crystalline, due to a very simple monomer structure, while PS and PC molecular motion is restricted due to benzene rings present in the monomer sidegroup and backbone, respectively.

B. Indentation, imaging, and image analysis

An instrumented nanoindenter (TriboIndenter, Hysitron Inc., Minneapolis, MN) collinear with a commercial scanning probe microscope or SPM (Quesant Inc., Agoura Hills, CA) was used to indent and acquire the load-depth or $P - h$ response of each sample and then to image the surface topography comprising each indentation at discrete time intervals over 48 h following the indentation experiment. The indenter was a diamond Berkovich (or trigonal pyramid) geometry of included semi-apex angle $\theta \sim 65°$ with nominal apex curvature (tip radius ~150 nm as quoted by the manufacturer and estimated via our nanoindentation of quartz). For calculated indentation volumes discussed below, an equivalent cone semi-apex angle of $\theta = 70.3°$ is assumed. To account for measurement drift caused by the piezoelectric actuator in the indenter transducer, each indentation experiment was initiated when this drift was ≤0.1 nm/s.

Each sample was tested in triplicate under load control to a specific maximum load P_{max} of 7 mN and, in separate experiments, to a specific maximum depth h_{max} of 1200 nm at constant loading and unloading rates of 0.5 mN/s. The latter experiment required material dependent maximum loads (PE: 1.6 mN, PC: 5 mN, PS: 7 mN). The resulting indentations were imaged in intermittent contact mode SPM with a Si cantilevered probe (CSC17; Quesant Inc., Agoura Hills, CA) of radius $r < 25$ nm over 48 h post-indentation t_o at discrete intervals (t_{SPM} = 4 min, 30 min, 1 h, 6 h, 12 h, 24 h, and 48 h). Piezoactuator drift normal to the sample surface that occurred between AFM images did not affect the applied analysis because depth values were calculated relative to a best-fit plane of the undeformed surface surrounding each indentation; this plane was determined individually for each image. Figure 1(a) compares the load-depth responses for PS, PC, and PE tested to the same h_{max}, indicating that PS is more resistant to contact loading than either PE or PC. Figure 1(b) shows the plan-view progression of the indentation surface recovery in PE, as measured via SPM over 48 h post-indentation.

Three-dimensional graphing and analysis software

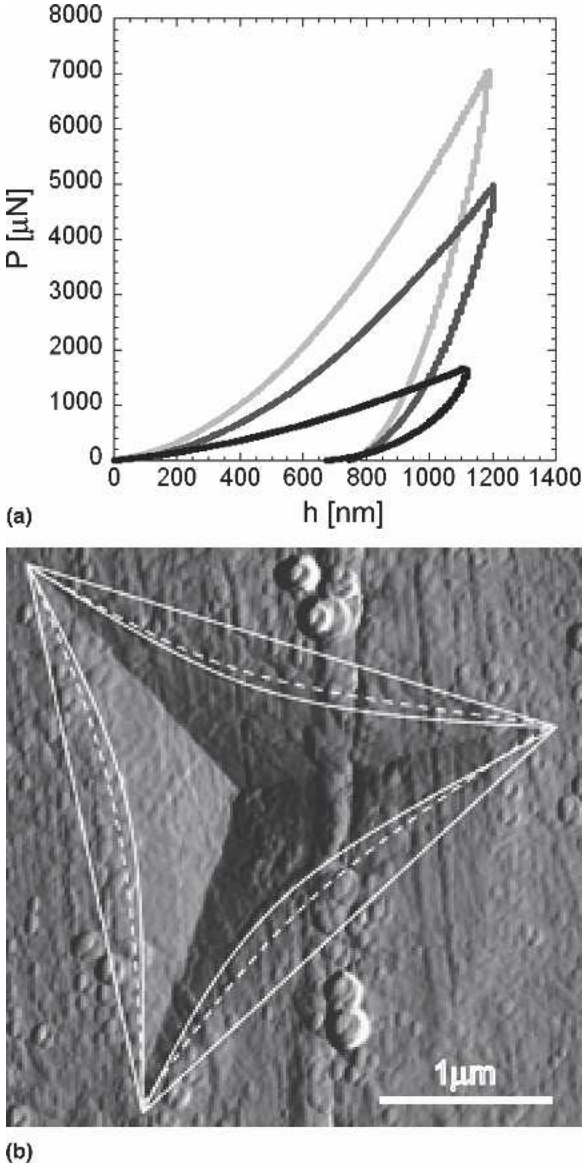

FIG. 1. (a) Load-displacement curves for indentations in polystyrene (light gray), polycarbonate (dark gray), and polyethylene (black) to approximately the same depth. (b) Tapping mode scanning probe microscopy amplitude image of an indentation in polyethylene to 7 mN at 48 h post-indentation. Sidewall bowing at the surface is delineated at the loss of contact (straight, solid lines), at 4 min (curved, dashed lines), and at 48 h (curved, solid lines) post-indentation.

(DPlot, Vicksburg, MS) was applied to SPM ASCII image data to determine the indentation depth minima (or nadir), $h_n(t)$, and to calculate the indentation volume, $V(t)$. For each image, indentation depth minima were calculated as the difference between the global minimum of all line scans and the averaged, tilt-corrected height of the undeformed surface surrounding the indentation. Indentation volumes were calculated by assigning the best-fit plane of the undeformed surface surrounding the indentation as $h = 0$ and then integrating over the indentation surface for all line scans. Although the first scan was executed immediately after each indentation ($t_{SPM} = 4$ min for each indentation), subsequent scans were acquired sequentially for indentations conducted in triplicate. Thus, temporal correspondence of acquisition times post-indentation differed by as much as 12 min for $t_{SPM} > 4$ min within an experimental condition, and reporting of averaged t_{SPM} and averaged calculated values would be misleading. Each recovery response $h(t)$ was fit separately to the viscoelastic model discussed below, and the standard deviation of h_n, V, and model parameters among triplicate experiments is reported in figures for the values of t_{SPM} stated previously.

In subsequent studies to consider recovery over $0 < t < 4$ min and the separate effects of loading time and unloading time on the extent of recovery, a hold segment at ($P_h = 100$ μN, $t_h = 60$ s) was introduced prior to full unloading to $P = 0$. The indentation depth $h_n(0 < t < 60$ s) was acquired directly from the upward displacement of the indenter. In the first set of these experiments, all three polymers were deformed to $h_{max} = 1200$ nm at a loading rate of 0.5 mN/s, duplicating the conditions of Fig. 1(a) that preceded sustained SPM imaging. In the second set of these experiments, PE was deformed to $h_{max} = 1200$ nm ($P_{max} = 1.6$ mN) at a loading rate of 0.5 mN/s, and the unloading rate was increased in a geometric series as 0.1, 0.5, or 2.5 mN/s. In the third set of these experiments, PE was deformed to $P_{max} = 1.6$ mN at a loading rate of 0.5 or 2.5 mN/s, and the unloading rate remained fixed at 0.5 mN/s.

III. RESULTS AND DISCUSSION

This systematic study of viscoelastoplastic indentation recovery facilitates consideration of two aspects of polymer characterization: prediction of the extent and timescales of recovery at deformed polymeric surfaces, and applicability of indentation hardness as a gauge of plastic deformation resistance.

A. Viscoelastic recovery progression

The progression of post-indentation recovery is shown in Fig. 2, for the case of polyethylene (PE) at $P_{max} = 7$ mN ($h_{max} = 2.64$ μm). In a typical indentation hysteresis, full recovery of the surface is assumed at $(P, h) = (0, h_o)$. However, upon unloading to a small positive load ($h_o + 100$ μN) as shown in Fig. 2(a), significant viscoelastic recovery of the indentation depth is measured via upward displacement of the nominally loaded surface over ~1 min post-indentation. In fact, consistent with linear viscoelastic models of recovery, the greatest recovery of indentation depth (~50% for PE) occurs in this interval. Subsequent SPM imaging of the indentation for $t > 4$ min (the time required for stage

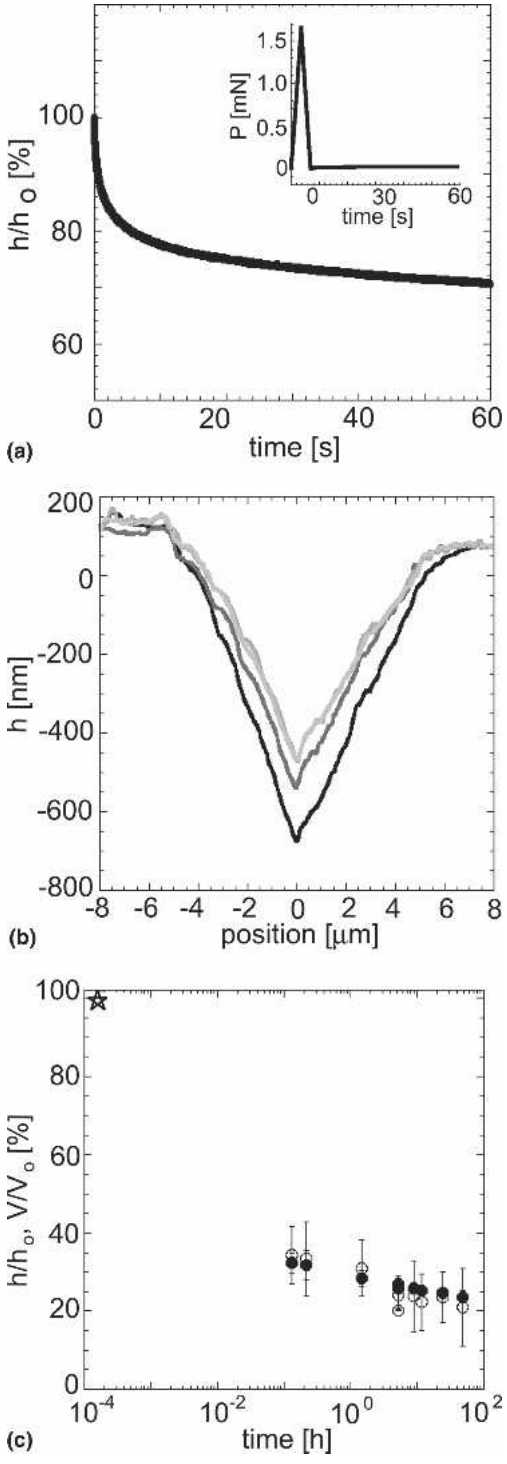

FIG. 2. Polymer surface recovery is detected immediately upon unloading via a low-load holding phase [loading profile pictured in inset of plot (a)]. (a) Normalized depth h/h_o recovery of polyethylene (PE) during hold segment after loading to 1.6 mN. (b) Scanning-probe microscopy line traces through the minimum of an indentation to 7 mN in PE at 4 min (black), 136 min (dark gray), 24 h (light gray), and 48 h (lightest gray). (c) Normalized depth h/h_o and volume V/V_o as a function of $t > t_o$ for PE loaded to 1.6 mN. Note that star represents h_o/h_o and V_o/V_o, which are measured and calculated via Eq. (4), respectively, from the last point of indentation unloading. Error bars represent standard deviation among triplicate experiments.

translation and initiation of SPM data acquisition) is shown in Fig. 2(b). This lagging recovery represents an additional ~25% decrease of the indentation depth between 4 min and 48 h post-indentation and, considered in conjunction with the indentation *P-h* response, is consistent with an instantaneous change in depth (extrapolation to $t = 0$) of ~50%. To confirm that this large, rapid change in h_n could not be attributed to calibration inaccuracies either in h_o as reported by the $P - h$ response of the instrumented nanoindenter or in h_n at $t = 4$ min as reported by the piezo-actuated SPM cantilever, additional experiments were conducted. First, we tested these three polymers under the same conditions with a different instrumented indenter for which indenter displacement can be independently calibrated as a function of displacement sensor voltage (NanoTest600, Micro Materials, Wrexham, UK) and found agreement with h_o within <4%. Second, we recalibrated the SPM displacement as a function of photodiode voltage with a 1 μm step standard and found agreement with the previous calibrations within <5%. Third, we considered a potential offset in the reference position of the undeformed surface between the nanoindenter and AFM, due to variation in contact force sensitivities (i.e., the indenter may displace the surface significantly before detecting contact). However, this disparity was much smaller than the magnitude of recoveries measured: the contact load of the indenter was 1 μN, corresponding to ≤3 nm of surface displacement prior to indentation data acquisition in these polymers. The plane fit to the undeformed regions of AFM images minimized the effect of nanoscale surface roughness, but RMS roughness was only 4–5 nm on these polymers. Thus, this significant recovery appears to accurately reflect the immediate post-indentation response of the deformed polymer volumes. Clearly, then, there exists a rapid recovery occurring immediately after loss of indenter contact that is not captured by the standard $P - h$ response.

Cross-sections through the minimum of the indentation volume demonstrated recovery of the indentation depth $h_n(t)$, as well as bowing of the indentation sidewalls [Fig. 2(b)]. For times $t \geq 4$ min post-indentation, only limited additional bowing of the sidewalls over 48 h was observed. Therefore, although the sidewall bowing predominantly transpired immediately following loss of indenter-material contact, the indentation depth recovered over at least 48 h.

The indentation topography afforded by SPM imaging also illustrates the evolution of volumetric recovery. The normalized recovery of indentation depth h_n/h_o and of indentation volume V/V_o is shown in Fig. 2(c). Here, instantaneous depth $h_n(t)$ and volume $V(t)$ were acquired via SPM, while h_o was acquired directly from the indentation $P - h$ response. If the indentation recovered as a self-similar volume of a cone, the corresponding volume

V_o could be inferred from idealized conical indenter geometry:

$$V_{o,\text{Berkovich}} = 8.2h_o^3 \quad . \tag{2}$$

However, as Fig. 2(b) illustrates, the apices remain fixed at least for 4 min < t < 48 h, and thus the volume corresponding to h_o may be expected to recover approximately as

$$V_{o,\text{Berkovich}} = 8.2h_{max}^2 h_o \quad . \tag{3}$$

The measured $h_n(t = 0)/h_o$ and calculated $V(t = 0)/V_o$ are unity at time $t = 0$ post-indentation. Although the instantaneous volume, V_o, cannot be measured experimentally, $V(t > 4$ min) calculated directly from the indentation SPM images confirms this proportional decrease in V_o and h_o, indicating that the indentation recovers not as a self-similar volume [Eq. (2)], but as a cone with constant base area and decreasing height [Eq. (3)]. This finding is in agreement with results such as Fig. 1(b), which indicate that the volumetric recovery due to sidewall bowing or apical contraction is negligible during the period captured via SPM. Therefore, from Fig. 2(b), it is apparent that that the indentation depth and volume recover at the same rate, such that:

$$V(t) = \left(\frac{1}{3}\pi R^2\right)h_n(t) \quad , \tag{4}$$

where R is the base-radius of the trigonal pyramidal indentation volume, at least for $t > 4$ min post-indentation.

B. Comparison among polymers and loading histories

Comparison of the volumetric recovery of these three polymers deformed to the same maximum depth and maximum volume [$P - h$ responses in Fig. 1(a)] is shown in Fig. 3(a). A clear material dependence of volumetric recovery from the $t = t_o$ conformation, ranging from 45% (PC) to 80% (PE), is exhibited over 48 h. As shown in Fig. 2(c) for PE, h/h_o recovers in the same manner as V/V_o for these polymers. The recovery of all three polymers can be approximated through nonlinear regression as a decaying exponential of the form

$$\frac{h_n(t)}{h_o} = c_1 + c_2 e^{-t/\tau} \quad , \tag{5}$$

where t here is time post-indentation and τ is the effective retardation time [Fig. 3(b)]. This is consistent with the recovery of a linear viscoelastic material approximated by a Kelvin model in series with a Maxwell model[14] (also termed a Burgers model[21]), where c_1 represents the normalized depth recovery at $t = \infty$ and $(c_1 + c_2)$ represents the normalized instantaneous depth recovery at $t = 0$. As implied by Fig. 3(b), PS and PC exhibited

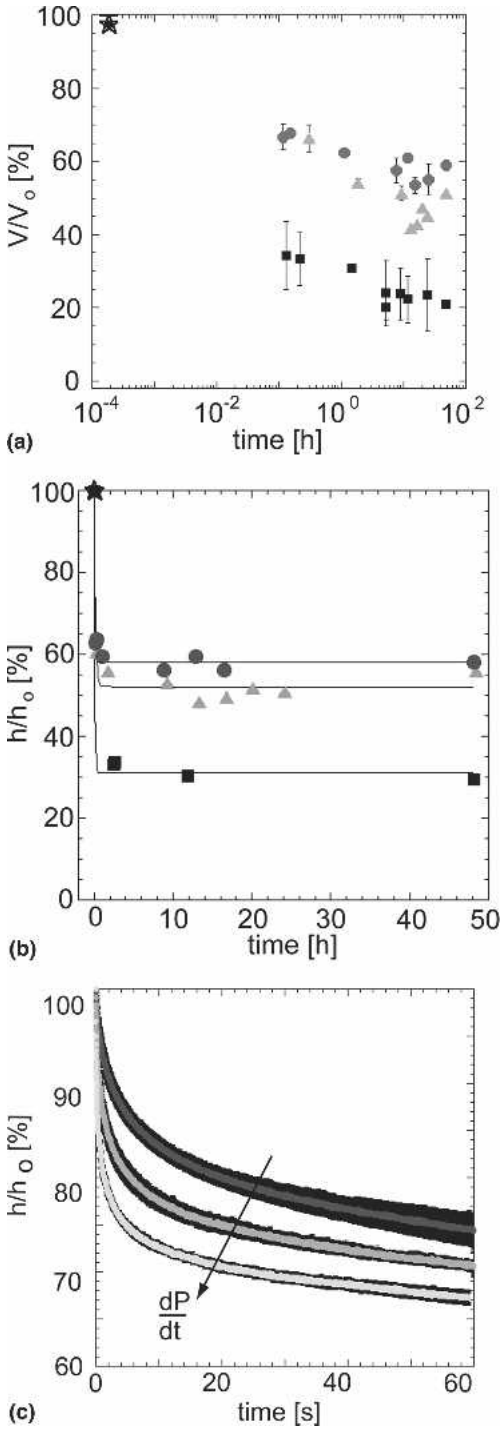

FIG. 3. (a) Normalized recovered volume V/V_o for indentations to $h_{max} = 1200$ nm in polyethylene (square), polystyrene (triangle), and polycarbonate (circle). (b) Normalized depth recovery of indentations to $P_{max} = 7$ mN in polyethylene (square), polystyrene (triangle), and polycarbonate (circle); decaying exponential or Burgers model fit shown as black lines. (c) Normalized depth h/h_o recovery in polyethylene during hold segment for three different unloading rates. The material was loaded to 1.6 mN at 0.5 mN/s and unloaded at 0.1 mN/s (dark gray), 0.5 mN/s (light gray), or 2.5 mN/s (lighter gray). Note that star represents V_o/V_o, where $V(t)$ is calculated via Eq. (4) from the last point of indentation unloading. Error bars represent standard deviation among triplicate experiments.

characteristic retardation times ($\tau = 10.94 \pm 0.57$ min and 5.69 ± 0.63 min, respectively) that were greater than those of PE ($\tau = 2.04 \pm 0.14$ min) for $P_{max} = 7$ mN. However, τ increased with increasing load for amorphous PC and decreased with increasing load for semicrystalline PE, indicative of the spectrum of recovery times in viscoelastic materials. More importantly, the rapidity of the decay illustrated in Fig. 3(b) indicates that the majority of viscoelastic recovery occurs over several minutes post-indentation, ranging from 70% for PE to 30% for PC, and is exhausted within 48 h at room temperature.

To further consider the effects of loading history on the extent and rate of viscoelastic recovery, we measured the upward displacement of the indenter upon unloading to $P = 100$ μN over 60 s post-indentation. This indenter displacement reflects the limited capacity of this indentation instrument to maintain load control (in open-loop), but is related directly to $h_n(0 < t < 60$ s) and results in a measurable increase in load P due to this material recovery. We found that the rate of instantaneous depth recovery assessed in this manner depended strongly on the magnitude of this dwell load. This rate appeared to be overestimated for small dwell loads due to the rapid recovery of the indentation sidewalls that forced the indenter to lose contact with the indentation depth minimum upon retraction from h_{max}, as well as to inertia of the piezo-actuated indenter during retraction from the surface. The measured extent of recovery was reduced by this counterloading of the recovering indentation, and thus the progression of $h_n(t < 4$ min) does not coincide quantitatively with $h_n(t > 4$ min). Nevertheless, we note that the ranking of the rapidity and extent of recovery among PS, PC, and PE deformed to the same h_{max} as observed during this dwell segment of recovery is consistent with that measured by SPM for 4 min $< t <$ 48 h.

As would be anticipated for a viscoelastic material under contact loading,[13] we observed that increased unloading time (decreased unloading rate) from a given P_{max} in PE correlated with decreased post-indentation recovery. As shown in Fig. 3(c), the increased viscous dissipation afforded by greater unloading time resulted in a statistically significant decrease in the extent of instantaneous recovery for a fixed loading rate of 0.5 mN/s. Here, geometric increases in unloading rate (0.1, 0.5, and 2.5 mN/s) correlated with increases in effective τ (0.12, 0.16, and 0.27 min, respectively); as noted previously, these τ are exaggerated due to volumetric contraction and expulsion of the indenter during unloading. In contrast, increased loading time to a fixed P_{max} and unloading time in PE resulted in a small but statistically significant increase in instantaneous recovery for loading rates greater than 0.5 mN/s (data not shown). Comparison of $h_n(0 < t < 60$ s) recoveries obtained for identical total times of indentation also indicated that decreases in unloading time more significantly affected this recovery progression than decreases in loading time (data not shown). Thus, the extent and progression of post-indentation viscoelastic recovery are more pronounced for decreased indentation loading/unloading times. This observation is particularly important with respect to the well-supported convention noted by Cheng and Cheng,[22] as well as others: rapid indentation unloading of a linear viscoelastic material enables reasonable estimation of the instantaneous elastic modulus. However, as a consequence of this rapid unloading, viscoelastic mechanisms and recoverable work that is measurable from the $P - h$ response are significantly suppressed.

C. Implications for indentation hardness of viscoelastic surfaces

These substantial recovery rates demonstrate the fleeting validity of indentation hardness H_i as a metric of plastic deformation resistance for polymers. Clearly, a decrease in h_n over time implies an increase in apparent resistance to permanent deformation. Therefore, if we assume a proportional decrease in contact depth h_c over time, H_i would change by at least 10% within 5 min (PE) to 3.5 days (PC) post-indentation for the range of common engineering polymers considered herein. As illustrated in the previous section, the extent of this error depends directly on loading and unloading times, and increases with loading rate. Thus, if hardness were used even as a quality control metric for which >10% accuracy may be acceptable, note that this error is in addition to that due to measurement precision, systematic analytical errors, and material inhomogeneities. Further, given that this effect is more pronounced for decreasing contact loads for a fixed loading rate, this inaccuracy increases for bulk or thin film polymers indented on the nanoscale—especially if such experiments also include conventional estimation of indentation elastic modulus via rapid unloading.[22] More importantly, H_i so quantified implies a resistance to plastic deformation that does not convey the observed, significant indentation depth recovery up to 80% within 2 days post-indentation. Although H_i should not and does not predict the extent of viscoelastic recovery, these results quantify the extent to which the common application of indentation $P - h$ response (related directly to H_i) fails to predict contact loading resistance afforded by viscoelasticity of polymeric surfaces.

As a result of this truncation of material response, the elastic or recoverable work of indentation W_e, calculable directly from integration of the $P - h$ response,[23] does not capture the total recoverable energy W_r at $t = \infty$. However, it cannot be assumed that the work recovered per unit material volume is constant during recovery, and

therefore it is not straightforward to analytically predict $W_r(t)$ from experimentally determined $h_n(t)$ or $V(t)$.

IV. CONCLUSIONS

In the present work, we have combined instrumented indentation and SPM imaging to formally demonstrate the significance and extent of post-indentation viscoelastic recovery in three common engineering polymers. For the range of indentation loads and rates considered, this recovery results in up to 80% recovery of indentation depth in excess of that measured from the instrumented indentation response. Consideration of a simple, linear viscoelastic model indicates that the extent and retardation time of this recovery vary significantly as a function of the physical/structural properties among these polymers, as well as of the preceding loading histories. Given the increasing application of instrumented indentation to quantify the resistance of (bio)polymeric surfaces to instantaneous loading (e.g., indentation elastic modulus E_i inferred through sufficiently rapid unloading and application of time-independent Oliver/Pharr-type analysis[5,22]) and permanent deformation (e.g., indentation hardness H_i calculated directly from the indentation hysteresis), this time-lapsed imaging of surface recovery illustrates two key points. First, the extent and rates of recovery depend directly on loading time, such that decreased loading time consistent with extraction of E_i from indentation hystereses implies significantly underestimated recoverable work and residual indentation depth. Second, despite the fact that H_i is a target metric for deformation resistance in a wide range of polymer applications including low-k dielectric coatings,[24] comparison among these polymers shows that this parameter is not only (un)loading time-dependent, but also that H_i is not even qualitatively predictive of which polymer is most resistant to permanent deformation. When the mechanical response of interest is best described as (contact) deformation resistance, careful consideration of the loading time with respect to the material retardation time or post-indentation imaging as presented herein is recommended. Although this particular sample set does not elucidate the specific structural determinants of the recovery energetics in confined polymer volumes, systematic consideration of these molecular constraints is in progress.

ACKNOWLEDGMENTS

We gratefully acknowledge Dr. G.S. Blackman for material samples and helpful discussion, as well as the DuPont-MIT Alliance for financial support. C.A. Tweedie acknowledges support though the National Defense Science and Engineering Graduate Fellowship program.

REFERENCES

1. M.R. VanLandingham, J.S. Villarrubia, W.F. Guthrie, and G.F. Meyers: Nanoindentation of polymers: An overview. *Macromol. Symp.* **167,** 15 (2001).
2. B.J. Briscoe and K.S. Sebastian: The elastoplastic response of poly(methyl methacrylate) to indentation. *Proc. R. Soc. London Ser. A* **452,** 439–457 (1996).
3. B.J. Briscoe, P.D. Evans, S.K. Biswas, and S.K. Sinha: The hardnesses of poly(methylmethacrylate). *Tribology International* **29,** 93 (1996).
4. C. Klapperich, K. Komvopoulos, and L. Pruitt: Nanomechanical properties of polymers determined from nanoindentation experiments. *J. Tribol-T Asme.* **123,** 624 (2001).
5. W.C. Oliver and G.M. Pharr: An improved technique for determining hardness and elastic-modulus using load and displacement sensing indentation experiments. *J. Mater. Res.* **7,** 1564 (1992).
6. B.T.A. Chang and J.C.M. Li: Indentation recovery of amorphous materials. *Scripta Metall Mater.* **13,** 51 (1979).
7. I.M. Low: Effects of load and time on the hardness of a viscoelastic polymer. *Mater. Res. Bull.* **33,** 1753 (1998).
8. V. Lorenzo, J.M. Perena, J.G. Fatou, J.A. Mendezmorales, and J.A. Aznarez: Delayed elastic recovery of hardness indentations in polyethylene. *J. Mater. Sci.* **23,** 3168 (1988).
9. V. Lorenzo, J.M. Perena, J.M.G. Fatou, J.A. Mendezmorales, and J.A. Aznarez: Interference microscopy measurements of depth at Vickers hardness indentations in polyethylene. *J. Mater. Sci. Lett.* **6,** 756 (1987).
10. B.T.A. Chang and J.C.M. Li: Indentation recovery of atactic polystyrene. *J. Mater. Sci.* **15,** 1364 (1980).
11. T.M. Kung and J.C.M. Li: Recovery processes in amorphous polymers. *J. Mater. Sci.* **22,** 3620 (1987).
12. F.Q. Yang, S.L. Zhang, and J.C.M. Li: Impression recovery of amorphous polymers. *J. Electron. Mater.* **26,** 859 (1997).
13. C.A. Tweedie, J.F. Smith, and K.J. Van Vliet: *Nanomechanics of Polymer Energy Absorption*, (Materials Research Society, Boston, MA, 2004).
14. R.J. Young and P.A. Lovell: *Introduction to Polymers* (Chapman & Hall, New York, 1991).
15. A. Brulet, F. Boue, and J.P. Cotton: About the experimental determination of the persistence length of wormlike chains of polystyrene. *J. Phys. II* **6,** 885 (1996).
16. J. Bicerano: Chain stiffness of liquid crystalline polyesters. 1. Characteristic ratio and persistence length. *Comput. Theor. Polym. Sci.* **8,** 9 (1998).
17. S. Nikolov and I. Doghri: A micro/macro constitutive model for the small-deformation behavior of polyethylene. *Polymer* **41,** 1883 (2000).
18. Y.G. Liu, S.Q. Bo, Y.J. Zhu, and W.H. Zhang: Studies on the intermolecular structural heterogeneity of a propylene-ethylene random copolymer using preparative temperature rising elution fractionation. *J. Appl. Polym. Sci.* **97,** 232 (2005).
19. F. Dinelli, G.J. Leggett, and P.H. Shipway: Nanowear of polystyrene surfaces: Molecular entanglement and bundle formation. *Nanotechnology* **16,** 675 (2005).
20. C.L. Soles, J.F. Douglas, W.L. Wu, and R.M. Dimeo: Incoherent neutron scattering as a probe of the dynamics in molecularly thin polymer films. *Macromolecules* **36,** 373 (2003).
21. L.E. Nielson: *Mechanical Properties of Polymers and Composites,* (Marcel Dekker, New York, 1974).
22. Y.T. Cheng and C.M. Cheng: Scaling, dimensional analysis, and indentation measurements. *Mater. Sci. Eng., R* **44,** 91 (2004).
23. M. Dao, N. Chollacoop, K.J. Van Vliet, T.A. Venkatesh, and S. Suresh: Computational modeling of the forward and reverse problems in instrumented sharp indentation. *Acta Mater.* **49,** 3899 (2001).

24. L.G. Wang, M. Ganor, S.I. Rokhlin, and A. Grill: Nanoindentation analysis of mechanical properties of low to ultralow-dielectric constant SiCOH films. *J. Mater. Res.* **20,** 2080 (2005).

APPENDIX: COMPARISON WITH MICROHARDNESS RECOVERY

Lorenzo et al. inferred an exponential dependence from plan-view, optical measurements of Vickers microindentation diagonal lengths and estimated μm-scale $h_n(t)$ in various polyolefins, at a single loading rate of 15 mN/s and loads exceeding those of the current study by at least twenty-fold. Consistent with their observations, we find that the percentage of depth recovery at short and long times can be predicted by assuming that at h_{max}, the indentation volume is well described by indenter geometry [Eq. (2), neglecting sink-in]. Thus, at any h_{max} for any material, the ratio R/h_{max} is a constant equal to 2.79 and Eq. (5) can be expressed in terms of R as

$$\frac{h_n(t)}{2R} = 0.18\,\frac{h_n(t)}{h_{max}} = \kappa_1 + \kappa_2 e^{-t/\tau} \quad , \qquad \text{(A1)}$$

where R is the contact radius at h_{max}, and the residual ($t = \infty$) and instantaneous ($t = 0$) recoveries of indentation depth can be determined directly from κ_1 and κ_2 as

$$\Delta h_n(t = \infty) = \frac{[0.18 - \kappa_1]}{0.18} \quad , \qquad \text{(A2a)}$$

$$\Delta h_n(t = 0) = \frac{[0.18 - \kappa_1 - \kappa_2]}{0.18} \quad . \qquad \text{(A2b)}$$

Through direct imaging of $h_n(t > 4$ min), the percentage of depth recovery we observed for PE at $P_{max} = 7$ mN (68 ± 1%) agrees reasonably well with that reported by Lorenzo et al. (76%) via optical interferometry for rapid Vickers microindentation in high-density polyethylene of approximately the same degree of crystallinity.[8] However, the instantaneous depth recovery (31 ± 8%) and retardation time (2.7 ± 0.01 min) we observed for these smaller indentations were considerably different from that reported by Lorenzo et al. (70% and 51 h, respectively). This may be attributable to material differences and to the comparatively underdeveloped plastic zone for our (twenty-fold) lower level of contact loading. Note that Chang et al.[10] applied a second order kinetic model to predict rate constants of recovery for microindentations near the glass transition temperature of amorphous polymers. In contrast, the recovery we measured at room temperature was not well described by second order kinetics.